BUBBLE DYNAMICS ON A HEATED SURFACE

M. Kassemi[1], N. Rashidnia[2], [1,2]NCMR, NASA LeRC, Cleveland OH 44135, Mohammad.Kassemi@lerc.nasa.gov, Nasser.Rashidnia@lerc.nasa.gov

INTRODUCTION

In this work, we study steady and oscillatory thermocapillary and natural convective flows generated by a bubble on a heated solid surface. Behavior of bubbles in terrestrial applications has been subject to extensive research especially as related to boiling processes. As a result, various procedures have been developed to minimize and control the problem of gas bubbles or exploit their properties on earth. In the microgravity environment, however, bubbles will behave in a significantly different manner and are expected to be more problematic. Therefore, understanding the intricacies of the Marangoni convection generated by bubbles is not only beneficial for terrestrial applications but may prove to be essential for controlling space processing experiments and interpreting their results.

The interaction between thermocapillary and natural convection flows can be very complicated. Experimental observations made in our Laboratory and those reported by other investigators[1] indicate that above a critical Ma number, the temperature and flow fields exhibit several complicated symmetric and asymmetric oscillatory modes. Previously, we studied the steady state thermocapillary and natural convection generated by a bubble on a heated solid surface in 1-g and low-g environments[2]. In this work, we focus on the transient flow and temperature fields generated by the bubble below and above the critical Ma number. It will be shown that below the critical Marangoni number, steady state conditions are attainable. In this situation, we compare the steady state numerical solutions predicted by our transient solver (by marching through time) with experimental results recently published by Wosniak and Wosniak[3].

Above the critical Marangoni number, we will show both numerically and experimentally that a symmetric oscillatory thermocapillary flow is generated by the bubble in 1-g. We will discuss the nature, origin, and dynamics of this oscillatory behavior in detail.

THEORETICAL BACKGROUND AND EXPERIMENTAL SETUP

Consider the enclosure containing a liquid (silicone oil) with a bubble injected and kept stationary at the inside of the top wall as shown in Fig. 1. The side walls are insulated and the temperature of the top and bottom walls are uniformly maintained at T_h and T_c, respectively. Therefore, a thermally stratified state is established in the enclosure before the bubble is introduced. Once the bubble is positioned and the interface between the air and the test liquid is formed, surface tension forces created by the temperature gradient along the interface will drive a thermocapillary convective flow. This thermocapillary flow disrupts the thermal stratification near the bubble resulting in significant temperature gradients and convection near the bubble surface.

The experimental setup designed and constructed to quantify the thermocapillary flow generated by the bubble consists of three main components; the test cell and the injector, the Mach-Zehnder Interferometer (MZI) or the Wollaston Prism Interferometer (WPI), and the laser sheet flow visualization unit. The onset of the thermocapillary and natural convection flows is determined by observing the interferometric fringe patterns created by the temperature field and visualizing the velocity field near the bubble using a laser sheet. A schematic of the test cell which is made of large optical glass widows suitable for interferometric measurements is shown in Fig. 2
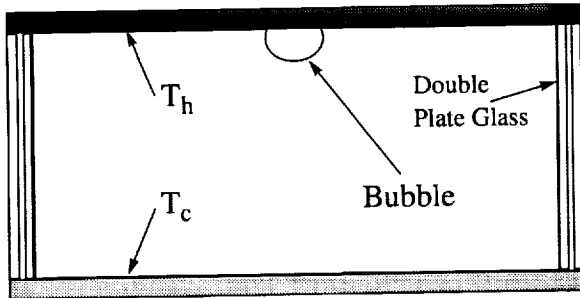
Figure 1. Schematic of The Test Enclosure.

Figure 2. Schematic of The Test Cell

A transient two-dimensional model is developed which describes the fluid flow and heat transfer induced by the bubble in terms of the continuity, momentum and energy equations. For details of the numerical and experimental procedures the reader is referred to Kassemi and Rashidnia[4].

RESULTS AND DISCUSSION

Steady State Results

In order to gain insight into the flow and temperature fields generated by the bubble, we first compare steady state solutions predicted by our transient numerical model with 1-g and low-g steady state experimental results provided by Wosniak and Wozniak[3] which are included in Figs. 3 and 4. Wozniak's reduced gravity results were obtained during the European TEXUS 33 sounding rocket experiments with low-gravity conditions of about 6 minutes duration.

The numerical simulations are generated by marching through time until steady state temperature and velocity fields are achieved. In the ground-based case, the numerical simulations are performed for Re = 4300, Gr = 2400, Pr = 122. Initially a hemispherical bubble shape is assumed by the model but the bubble shape changes very fast to accommodate the forces exerted upon it. At 1g, due to the presence of the large hydrostatic force, the steady state bubble shape predicted by the model, is much flatter than its originally assumed exact hemispherical shape. In this case, because of the simultaneous action of the buoyancy and thermocapillary forces, a vigorous thermocap-

illary vortex coexists with two weaker vortices below the bubble as shown by the streamlines in Fig. 5. The strongest vortex driven by the thermocapillary force fills the top portion of the enclosure next to the bubble. It carries the fluid down along the surface of the bubble creating a strong boundary layer flow which is revealed by the packing of streamlines near the interface. The temperature contours around the bubble are moderately distorted by this flow as indicated in Fig 5. The steady state bubble shape and temperature and fluid fields (which prevail at t=180s and beyond) are in excellent agreement with the steady state results of Wozniak reproduced in Fig. 3a.

Next, conditions pertinent to Wozniak's microgravity experiment are considered for g = $10^{-4}g_o$, Ma = 1830, Ra = 0.25, Pr = 122. Note that a vigorous thermocapillary flow is generated next to the bubble surface. But in contrast to the terrestrial examples presented in Fig. 5, this time a natural convective flow will not ensue due to the reduced buoyancy force. As a result, the recirculating thermocapillary vortex will grow unopposed until it nearly fills the entire enclosure at steady-state. The streamlines of Fig. 6 clearly show that the microgravity flow pattern resembles a jet-like flow emanating from around the bubble and flowing downwards into the enclosure. As a result of this intense recirculating flow, the temperature field is greatly altered. Again, there is excellent agreement between our numerical predictions and the experimental results of Wozniak for bubble shape and the velocity and temperature profiles even though
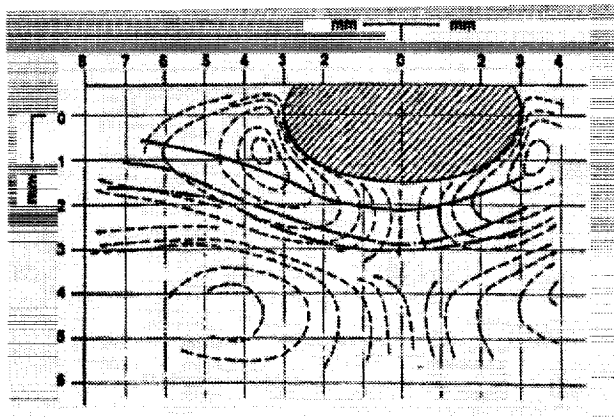
Figure 3. 1-G Experimental Temperature and Streamline Contours for Ma = 2440, Ra= 500, and Pr=122 (Wozniak and Wozniak[3]).
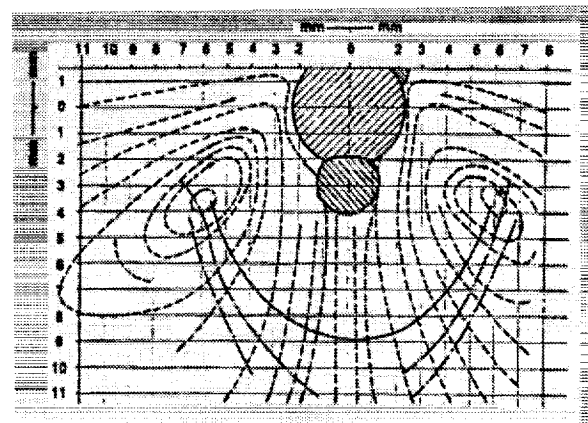
Figure 4. Low-G Experimental Temperature and Streamline Contours for Ma = 1830, Ra= 0.25, and Pr=122 (Wozniak and Wozniak[3]).

a) Streamlines
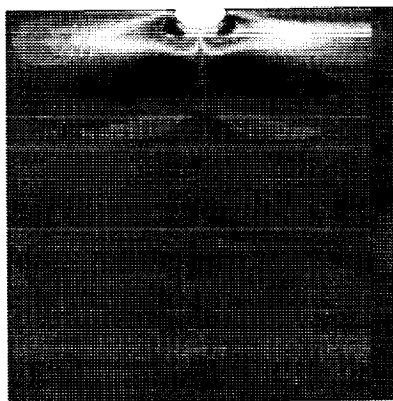
b) Temperature Contours
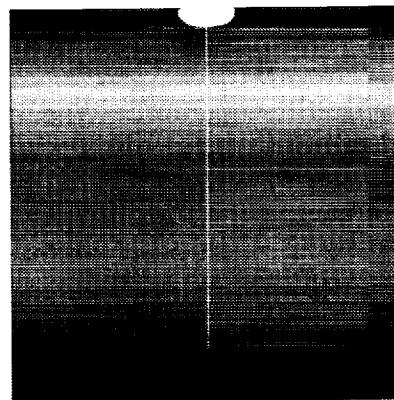
Figure 5. 1-G Numerical Predictions of a) Streamlines, b) Temperature Contours, and Bubble Shape for Ma=2440, Ra=500, and Pr=122 at t=180s.

a) Streamlines
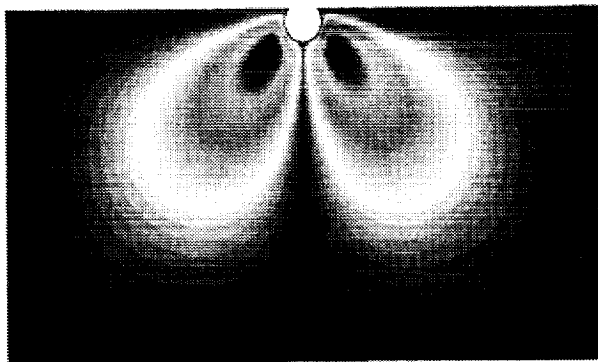
b) Temperature Contours
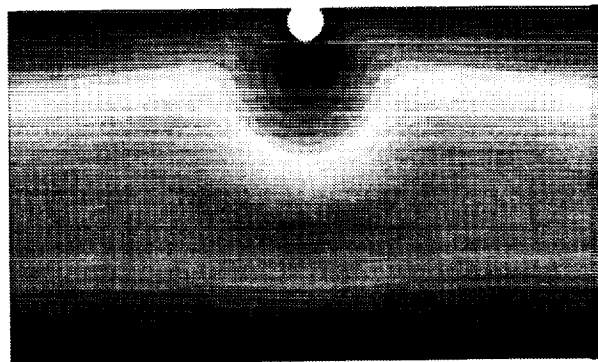
Figure 6. Low-G Numerical Predictions of a) Streamlines, b) Temperature Contours, and Bubble Shape for Ma=1830, Ra=0.25, and Pr= 122 at t=200s.

90

Temperatutre-Time History
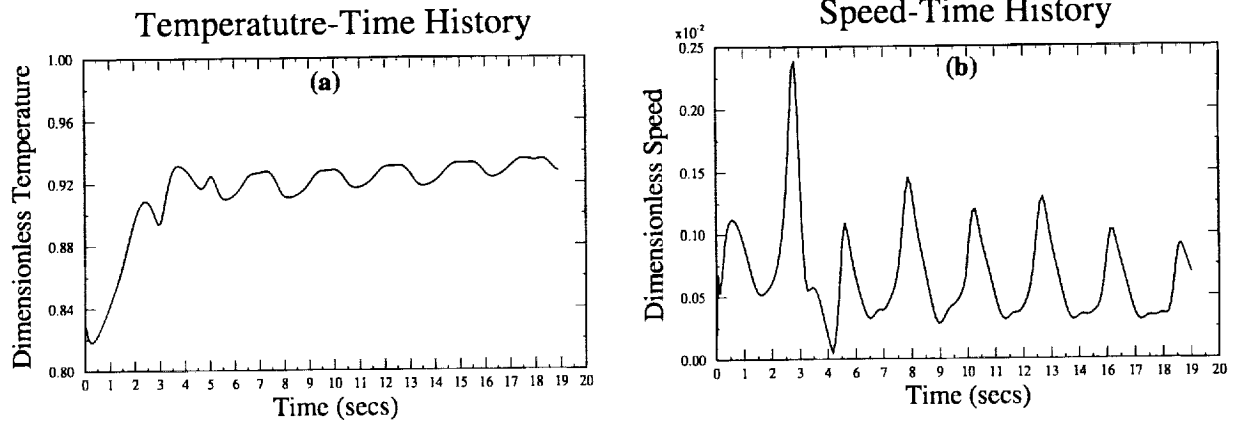
Speed-Time History

Figure 7. Temperature-Time History (a) and Velocity-Time History (b) of a Point on the Bubble Surface for Ma= 90,000, Ra=50,000, and Pr=8.4.

during the low gravity experiment an unexpected smaller bubble formed and remained attached to the larger bubble.

Unsteady Flows Beyond The Critical Ma Number

Experiments performed in our laboratory indicate that beyond a critical Ma of approximately 12,000 the flow and temperature fields undergo several oscillatory modes depending on the value of the Ma number. The interferograms (presented in Fig. 8a) show the oscillatory temperature field which occurs at Ma = 90,000, Ra = 20,000, Pr=8.4. The oscillations are symmetric and are accompanied by an up and down periodic motion in the fluid.

The temperature-time and velocity-time history of a point on the bubble surface obtained during the numerical simulation of the high Ma number case are presented in Fig. 7. In this situation, the flow and temperature fields develop much along the same lines as the 1-g low Marangoni case discussed previously but at around 6s, because of the strength of the convection, the velocity and temperature fields go into a periodic oscillatory mode. The numerical simulations of this high Marangoni case show an intricate interplay between heat and momentum transfer as depicted in Figs. 8b-c and 19a-b for one period of oscillation. Figs. 8b and c show that initially at t = 0, the vigorous thermocapillary vortex which is near the lower portions of the bubble brings the hot fluid down the surface of

the bubble while taking the colder fluid from the inner regions of the enclosure up into an area close to the bubble. This flow will modify the temperature field drastically creating a cold finger near the bubble surface as shown in Fig. 8b (t = 2π/5-6π/5). This cold finger is the main cause of the instability. The corresponding interfacial temperature and velocity distributions are presented in Fig. 9 for one period of oscillation. At the beginning of the cycle t = 0, the temperature drops drastically near the hot wall and then monotonically decreases at a much smaller slope as the top of the bubble is approached. The interfacial velocity also achieves its maximum in the high temperature gradient region near the hot wall and monotonically decreases to zero as the top of the bubble is approached. As the cold finger forms and grows (t = 2π/5-6π/5), touching the bubble interface, it perturbs the interfacial temperature profile by creating a temperature dip on the surface. This increases the tangential temperature gradient in the base region as shown in Fig. 9a and creates a gradient reversal further down along the interface. Fig. 9b shows that as a result of this temperature dip, the fluid velocity is reduced to zero for a good portion along the bubble surface. The net effect of these changes is to push the center of the thermocapillary vortex up towards the hot wall as shown at t = 4π/5-6π/5 in Fig. 8c. At this new location, the vortex will draw from the warmer fluid near the hot wall which to-

91

a) Sequence of Interferogram Fringe Patterns around The Bubble During One Period of Oscillation

| 0 | $2\pi/5$ | $4\pi/5$ |
| $6\pi/5$ | $8\pi/5$ | 2π |
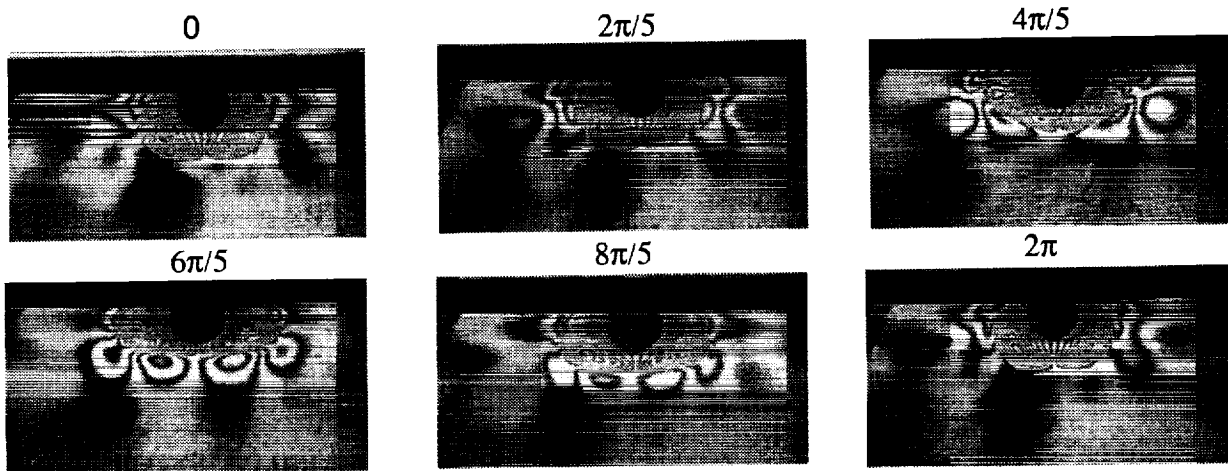
b) Numerical Predictions of Temperature Contours around The Bubble During One Period of Oscillation

| 0 | $2\pi/5$ | $4\pi/5$ |
| $6\pi/5$ | $8\pi/5$ | 2π |
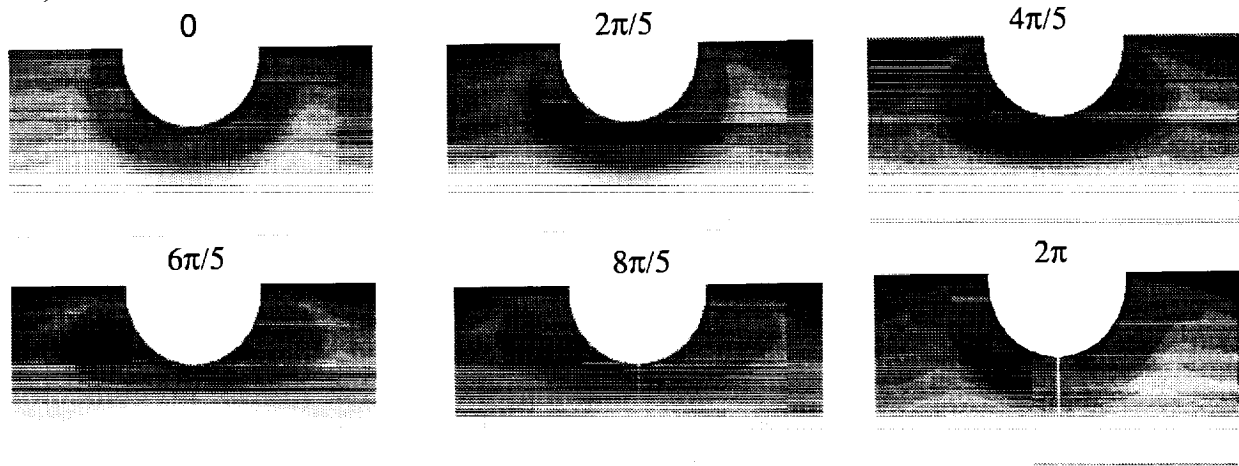
c) Numerical Predictions of Streamline Contours During One Period of Oscillation in The Entire Enclosure

| 0 | $2\pi/5$ | $4\pi/5$ |
| $6\pi/5$ | $8\pi/5$ | 2π |
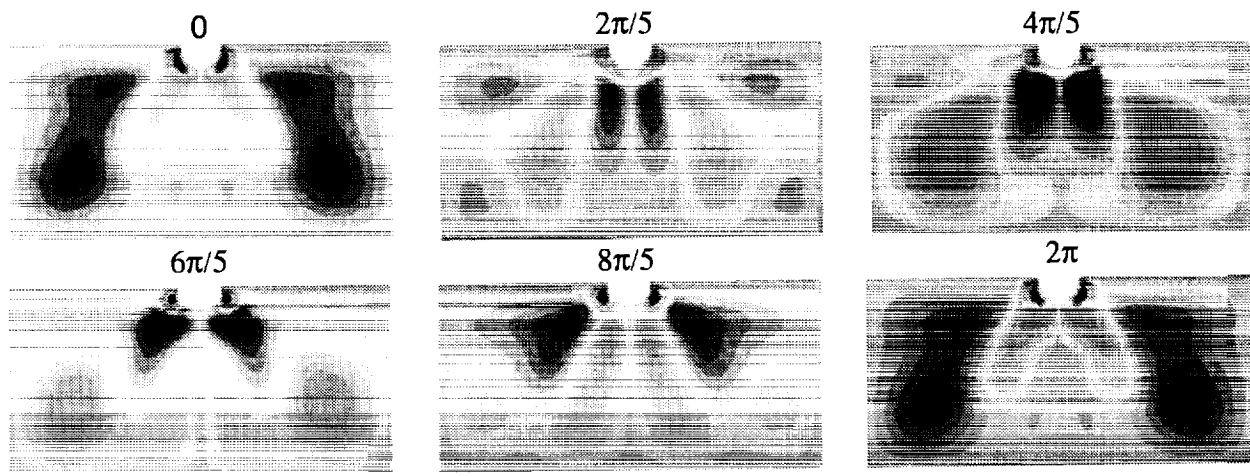
Figure 8. 1-G a) Experimental Interferograms (WPI) and Numerical Predictions of b) Temperature and c) Streamline Contours During One Period of Oscillation for Ma=90,000, Ra=50,000, and Pr= 8.4.
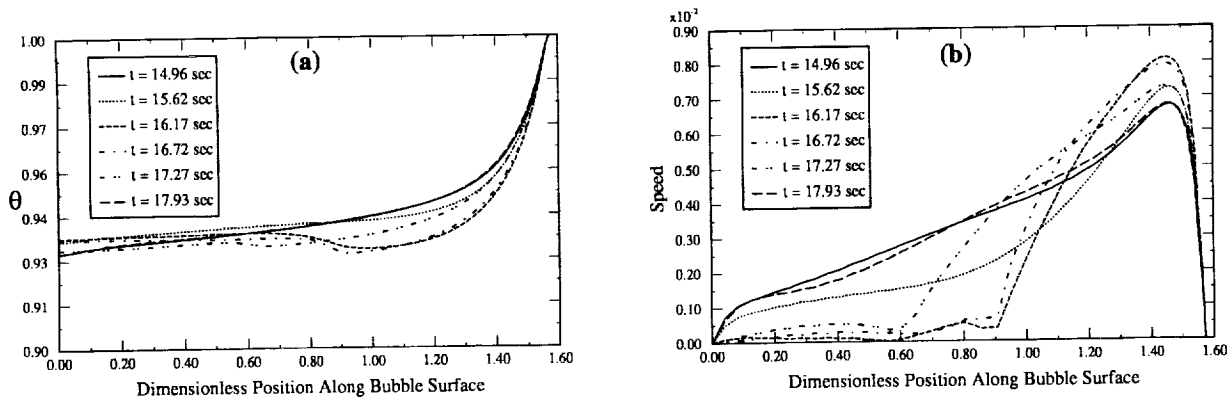
Figure 9. Interfacial Temperature (a) and Velocity (b) Profiles During One Period of Oscillation for Ma= 90,000, Ra=50,000, and Pr=8.4 (The Origin Corresponds to The Intersection of Bubble with The Centerline).

gether with the vigorous mixing action will tend to gradually diminish the cold finger as shown in time sequences $8\pi/5$-2π. As the cold finger diminishes, the temperature dip on the bubble surface disappears, relaxing temperature gradients near the base and increasing the velocity along the bubble surface. Finally, at t = 2π, the thermocapillary vortex returns to its original position near the base of the bubble and one period of oscillation is completed. The streamline contours of Fig. 8 show that this complex interplay between transport of heat and momentum results in a virtual pumping action first pushing down and then pulling up the fluid from below the bubble.

CONCLUSIONS

In this work a combined experimental-numerical approach is adopted to investigate the steady and oscillatory fluid flow and temperature fields created by a bubble attached to a heated solid surface. Both experimental observation and numerical predictions indicate that the thermocapillary flow induced by bubbles on earth is greatly influenced and affected by its inevitable interactions with buoyancy-driven convection. Below the critical Marangoni number, the steady state low-g and 1-g temperature and velocity fields predicted by the finite element model are in excellent agreement with both visualization experiments in our laboratory and recently published experimental results in the literature. Above the critical Marangoni number, the model predicts an oscilla-

tory flow which is also closely confirmed by experiments. It is shown that the dynamics of this oscillatory flow are directly controlled by the thermal and hydrodynamic interactions brought about by combined natural and thermocapillary convection. Therefore, as the numerical simulations show, there are considerable differences between the 1-g and low-g temperature and flow fields at both low and high Marangoni numbers. This has serious implications for both materials processing and fluid management in space.

ACKNOWLEDGMENT

REFERENCES

1. Raake, D., Siekmann, J., Chun, CH.-H., *Temperature and Velocity Fields Due to Surface Tension Driven Flow*, **Experiments in Fluids**, Vol. 7, pp. 164-172, 1989.

2. Kassemi. M. and Rashidnia, N., *Thermocapillary and Natural Convective Flows Generated by a Bubble in 1-G and Low-G Environments*, Technical Paper AIAA 96-0743, 1996.

3. Wozniak, G. Wozniak, K., and Bergelt, H., *On the Influence of Buoyancy on the Surface Tension Driven Flow around a Bubble on a Heated Wall*, **Experiments in Fluids**, Vol. 21, pp. 181-186, 1996.

4. Kassemi. M. and Rashidnia, N., *Steady and Oscillatory Flows Generated by a Bubble in 1-G and Low-G Environments*, Technical Paper AIAA 97-0924, 1997.